Pacific Northwest
NATIONAL LABORATORY

PNNL-29612

Regional Oscillation Source Localization

Implementation in the ESAMS Tool

January 2020

Jim Follum
Tianzhixi (Tim) Yin
Nicholas Betzsold

U.S. DEPARTMENT OF ENERGY

Prepared for the U.S. Department of Energy
under Contract DE-AC05-76RL01830

DISCLAIMER

PACIFIC NORTHWEST NATIONAL LABORATORY
operated by
BATTELLE
for the
UNITED STATES DEPARTMENT OF ENERGY
under Contract DE-AC05-76RL01830

Printed in the United States of America

Available to DOE and DOE contractors from the
Office of Scientific and Technical Information,
P.O. Box 62, Oak Ridge, TN 37831-0062;
ph: (865) 576-8401
fax: (865) 576-5728
email: reports@adonis.osti.gov

Available to the public from the National Technical Information Service
5301 Shawnee Rd., Alexandria, VA 22312
ph: (800) 553-NTIS (6847)
email: orders@ntis.gov <https://www.ntis.gov/about>
Online ordering: http://www.ntis.gov

PNNL-29612

Regional Oscillation Source Localization

Implementation in the ESAMS Tool

January 2020

Jim Follum
Tianzhixi (Tim) Yin
Nicholas Betzsold

Prepared for
the U.S. Department of Energy
under Contract DE-AC05-76RL01830

Pacific Northwest National Laboratory
Richland, Washington 99354

Abstract

In recent years, utilities have made great strides in the use of high-speed wide-area measurements collected from within their footprints. However, it is increasingly clear that analyses at wider scales are needed. On January 11, 2019 an oscillation with significant amplitude observable across the Eastern Interconnection persisted for approximately 18 minutes. The generator responsible for the oscillation was only identified after it tripped itself offline. This event, along with several other similar events, demonstrated the need for increased coordination among utilities to effectively mitigate system-wide oscillations and avoid unnecessary or detrimental operator actions. In response to this need, the Eastern Interconnection Situational Awareness Monitoring System (ESAMS) was upgraded to allow the region where an oscillation is originating to be identified. This report documents the algorithms developed for this task and describes how they were integrated into the ESAMS tool. Results from simulation- and measurement-based tests demonstrate the reliability of the approaches.

Acknowledgments

The authors would like to thank Ali Ghassemian, Sandra Jenkins, and the rest of the Transmission Reliability Program under the Department of Energy's Office of Electricity for the sponsorship of this research effort. The authors gratefully acknowledge Slava Maslennikov of ISO-NE and Daniel Trudnowski of Montana Tech for their helpful guidance in developing and testing the methods described in this report. The authors also acknowledge the staff of PJM, ISO-NE, Dominion Energy, and the Bonneville Power Administration for providing measurements, models, and feedback that were essential in testing and refining the algorithms. We also thank Ken Martin and Simon Mo of EPG for their collaboration on the ESAMS tool and Joe Eto of Lawrence Berkeley National Laboratory for coordinating the ESAMS team.

Acronyms and Abbreviations

DEF	Dissipating Energy Flow
DFT	Discrete Fourier Transform
EI	Eastern Interconnection
EIDSN	Eastern Interconnection Data Sharing Network
ESAMS	Eastern Interconnection Situational Awareness and Monitoring System
ISO-NE	Independent System Operator of New England
PMU	Phasor Measurement Unit
WECC	Western Electricity Coordinating Council

Contents

Abstract.....ii
Acknowledgments.....iii
Acronyms and Abbreviations.....iv
Contents.....v
1.0 Introduction.....6
2.0 A New Formula for Dissipating Energy Flow.....7
3.0 Regional Oscillation Source Localization.....11
4.0 ESAMS Implementation.....18
5.0 Conclusion.....20
6.0 References.....21

Figures

Figure 1. Conceptual illustration of regional oscillation source localization.....12
Figure 2. One-line diagram of the 179-bus model with seven defined regions.....13
Figure 3. Simplified map of the ISO-NE system.....16
Figure 4. Diagram of the ESAMS tool.....18

Tables

Table 1. Results of the regional oscillation source localization algorithm applied to simulated natural oscllation cases.....14
Table 2. Results of the regional oscillation source localization algorithm applied to simulated forced oscllation cases.....15
Table 3. Results of the regional oscillation source localization algorithm applied to measured oscllation cases.....17

1.0 Introduction

Beginning in 2008, the U.S. Department of Energy's Smart Grid Investment Grant Program led to the deployment of an advanced measurement infrastructure throughout the country's power system. This infrastructure is based largely on synchrophasor technology, which provides high-speed, time-synchronized measurements over wide areas. In subsequent years, software vendors produced a variety of tools to support the use of synchrophasors in operations and planning. As a result, it is now common for utilities to use measurements from within their footprint to perform tasks such as model validation, diagnosis of equipment malfunction, and oscillation monitoring. While use of synchrophasors has grown, it remains relatively uncommon for measurements from multiple entities to be analyzed together to achieve a wide-area view across an interconnection. The research reported here is part of an effort to demonstrate the value of sharing measurement data across utility boundaries in the U.S. Eastern Interconnection (EI).

The research effort will culminate with the deployment of the prototype Eastern Interconnection Situational Awareness and Monitoring System (ESAMS). The tool will analyze measurements from several system operators and generate reports highlighting unusual power system conditions. The analytics within ESAMS are specifically targeted at conditions of concern at the interconnection level: wide-area voltage angle separation and system-wide sustained oscillations. As discussed in (NASPI Control Room Solutions Task Team 2016), changes in the separation between areas of the system, as measured by their voltage angles, can serve as precursors to severe problems. For this reason, the project team developed new methods to identify when voltage angle pairs across the system become abnormal (Amidan, et al. 2018). The focus of the present report is on new developments in monitoring and addressing system-wide sustained oscillations.

On January 11, 2019, an event occurred in the EI that clearly demonstrated the need for improved monitoring and mitigation strategies for oscillations. As detailed in (Fritch 2019), the oscillation originated in Florida due to equipment malfunction at a thermal generating site. Significant swings in power, voltage, and frequency were observed across the EI for approximately 18 minutes until the plant eventually tripped offline. Several utilities detected the oscillation while it was occurring, but it was only after the oscillation ceased that the source was identified. The January 11 event underscored the need for better coordination among utilities during system-wide oscillatory behavior. To support this coordination, ESAMS was equipped with new methods to identify an oscillation's source region using synchrophasor measurements from across an interconnection. This report describes these new methods in detail.

The remainder of the report is organized as follows. Section 2.0 describes the background and recent advancements of the algorithm traditionally used to identify an oscillation's source within a utility's footprint. Section 3.0 then discusses how the algorithm can be used at the interconnection scale to identify the region containing the oscillation's source. The implementation within ESAMS is detailed in Section 4.0. Finally, a discussion of current challenges and expected future work is provided in Section 5.0.

2.0 A New Formula for Dissipating Energy Flow

The widespread deployment of synchrophasor networks led to the observation that sustained oscillations occur in power systems with more regularity than previously understood. In response, a wide array of synchrophasor-based methods for identifying an oscillation's source were developed (Wang and Sun 2017). Oscillation source identification is a challenging problem due to the complexity of power systems and the variety of conditions that can lead to an oscillation. In particular, the inherent dynamics of power systems can create oscillations that are largest far from their source. To thoroughly evaluate the many methods being proposed the authors of (Maslennikov, Wang and Zhang, et al. 2016) developed a public test case library containing a variety of oscillation examples. The dissipating energy flow (DEF) method that serves as the basis for the present work was found to provide consistently reliable results using the test case library (Maslennikov, Wang and Litvinov 2017).

The DEF method was first proposed in (Chen, Min and Hu 2013). It operates by calculating the flow of dissipating transient energy through the power system network using synchrophasor measurements. The system component producing energy (positive DEF) is identified as the oscillation source. Components absorbing energy have a negative DEF. The method was later refined for practical use by band-pass filtering measurements at the frequency of the oscillation (Maslennikov, Wang and Litvinov 2017). To maintain practicality while avoiding the challenges of designing and applying filters in the online environment, ESAMS uses a new frequency-domain implementation of the DEF method. A derivation for this method is provided in the remainder of this section. The derivation was previously published in (Follum 2020).

The measurements required for the DEF method are active power, reactive power, system frequency, and voltage magnitude. Each of these measurements can be produced by a phasor measurement unit (PMU). Denote the measurements of active power as

$$P(t) = P_s + P_f(t) \tag{2.1}$$

where P_s is the steady-state term and the oscillation term is

$$P_f(t) = A_P \cos\left(\omega_f t + \theta_P\right). \tag{2.2}$$

Here A_P, ω_f, and θ_P are the amplitude, frequency in radians per second, and phase of the oscillation. Note that the oscillation is represented here as a single sinusoid. Most sustained oscillations in power system arise due to a periodic disturbance, e.g., a steam valve cycling between open and closed. This results in oscillations that are well-represented by a sum of sinusoids at harmonic frequencies. For the initial development only one sinusoid is considered. As discussed later in this section, practical implementation of the derived algorithm addresses harmonics and additional sinusoids.

Following the model for active power, let $Q(t) = Q_s + Q_f(t)$, $\Omega(t) = \Omega_s + \Omega_f(t)$, and $V(t) = V_s + V_f(t)$ denote measurements of reactive power, system frequency in radians per second, and voltage magnitude. The oscillation components of these measurements have the same form as (2.2). To simplify notation, the dependence on time of the oscillation components will be omitted for the remainder of the report, i.e., $P_f(t) = P_f$.

The DEF can be expressed in terms of power system quantities as (Chen, Min and Hu 2013, Maslennikov, Wang and Litvinov 2017)

$$W = \int P_f d(\theta_f) + \int Q_f d(U_f) \tag{2.3}$$

where θ_f denotes the oscillation component of the voltage angle and U_f denotes the oscillation component of

$$U(t) = \ln(V(t)). \tag{2.4}$$

The methods proposed in (Chen, Min and Hu 2013, Maslennikov, Wang and Litvinov 2017) estimate the DEF by directly evaluating the integrals in (2.3) with discrete approximations. In the following, a new expression for the DEF is obtained by simplifying (2.3) considering the sinusoidal nature of the terms.

To begin, note that because P_f, θ_f, Q_f, and U_f are all functions of time, the integrals can be rewritten as

$$W = \int_0^T P_f \Omega_f dt + \int_0^T Q_f U_f' \, dt \tag{2.5}$$

where T is the analysis length in seconds and $'$ indicates the first derivative. Assume the analysis length is selected to contain an integer number of oscillation cycles. To obtain an expression for U_f', note that

$$\begin{aligned} U(t) &= \ln\left(V_s + A_V \cos(\omega_f t + \theta_V)\right) \\ &\approx \ln(V_s) + \frac{A_V}{V_s}\cos(\omega_f t + \theta_V) \end{aligned} \tag{2.6}$$

for $V_s \gg A_V$ (see the appendix of (Follum 2020) for justification). Letting,

$$U_s = \ln(V_s) \tag{2.7}$$

$$A_U = \frac{A_V}{V_s} \tag{2.8}$$

$$\theta_U = \theta_V \tag{2.9}$$

leads to

$$\begin{aligned} U(t) &= U_s + A_U \cos(\omega_f t + \theta_U) \\ &= U_s + U_f(t). \end{aligned} \tag{2.10}$$

The derivative of the oscillation component follows as

$$U_f' = -\omega_f A_U \sin(\omega_f t + \theta_U). \tag{2.11}$$

With each term in (2.5) expressed as a sinusoid, the expression for the DEF can be greatly simplified. Applying the trigonometric identity

$$\cos(\alpha)\cos(\beta) = \frac{1}{2}\cos(\alpha-\beta) + \frac{1}{2}\cos(\alpha+\beta), \tag{2.12}$$

The first integral can be written as

$$\int_0^T P_f \Omega_f dt = \frac{T}{2} A_P A_\Omega \int_0^T \left[\cos(\theta_P - \theta_\Omega) + \cos\left(2\omega_f t + \theta_P + \theta_\Omega\right)\right]. \tag{2.13}$$

Noting that the integral of a sinusoid over an integer number of periods is equal to zero,

$$\int_0^T P_f \Omega_f dt = \frac{T}{2} A_P A_\Omega \cos(\theta_P - \theta_\Omega). \tag{2.14}$$

Similarly, applying the trigonometric identity

$$\cos(\alpha)\sin(\beta) = \frac{-1}{2}\sin(\alpha-\beta) + \frac{1}{2}\sin(\alpha+\beta) \tag{2.15}$$

allows the second integral to be expressed as

$$\int_0^T Q_f \mathrm{U}_\mathrm{f}^{'}\, dt = \frac{T}{2} A_Q A_\mathrm{U} \omega_f \sin\left(\theta_Q - \theta_U\right). \tag{2.16}$$

Combining the results in (2.14) and (2.16) leads to the final expression

$$W = \frac{T}{2}\left[A_P A_\Omega \cos(\theta_P - \theta_\Omega) + A_Q A_\mathrm{U} \omega_f \sin\left(\theta_Q - \theta_U\right)\right]. \tag{2.17}$$

To estimate the DEF using this expression, each amplitude and phase must first be estimated. Multiple approaches could be used for this task. In the following, a simple method based on the Discrete Fourier Transform (DFT) is proposed.

Before proceeding, note that the measurements used to estimate the DEF are sampled at a regular interval. Thus, discrete-time notation is introduced here for use in the following derivation. Let $k = 0,1,\ldots,K-1$ denote the sample indices within the analysis window corresponding to a sampling period T_s such that $t = k \times T_s$. Further, let $\omega^k = \omega \times T_s$ denote frequency in radians per sample.

Let $\tilde{P}_f\left(\omega^k\right)$ denote the DFT of $P_f(k)$. An estimate of this DFT at the oscillation frequency can be obtained as

$$\widehat{\tilde{P}}_f\left(\omega_f^k\right) = DFT\{P(k) - P_\mu\}|_{\omega^k = \omega_f^k} \tag{2.18}$$

where P_μ denotes the average of $P(k)$ over the analysis window. Because $P_f(k)$ is a cosine, it follows that

$$\tilde{P}_f\left(\omega_f^k\right) = \frac{K}{2} A_P \angle\theta_P. \tag{2.19}$$

Thus, estimates of the amplitude and phase of the oscillation as observed in active power measurements can be expressed as

$$\widehat{A}_P = \frac{2}{K}\left|\widehat{\widetilde{P}}_f\left(\omega_f^k\right)\right| \tag{2.20}$$

$$\widehat{\theta}_P = \angle\widehat{\widetilde{P}}_f\left(\omega_f^k\right). \tag{2.21}$$

Similar relationships hold for the other measured quantities. Thus, amplitude and phase estimates can be obtained by removing the mean from each set of measurements, calculating the DFT, and finding the magnitude and phase at the frequency of the oscillation. These estimates are then plugged into (2.17) to estimate the DEF.

Because the method operates in the frequency domain, the bandpass filtering prescribed in (Maslennikov, Wang and Litvinov 2017) is unnecessary. This is advantageous because filtering necessarily distorts a portion of the input signal that must then be truncated. Further, the filter design must be automated to account for the oscillation frequency. This does not provide the user an opportunity to validate the filter's design for performance and sensitivity. By operating in the frequency domain, the method can also evaluate oscillations at multiple frequencies simultaneously. The performance of the proposed DEF estimator was evaluated thoroughly and shown to perform similarly to the direct approach proposed in (Maslennikov, Wang and Litvinov 2017). Detailed results are provided in (Follum 2020). In the following section, the DEF estimation algorithm is used to support a new method of localizing an oscillation to its source region.

3.0 Regional Oscillation Source Localization

Presently, there is little coordination among system operators during an oscillation event. This was clearly demonstrated during the January 11 event in the EI. Even if utilities have operating procedures in place for oscillations and communicate with neighboring entities over phone lines, there is currently no strategy for identifying the source of an oscillation at the interconnection level. The methods described in this section could be used to support the implementation of such a strategy.

The proposed method is actually an extension of an approach already in use at the Independent System Operator of New England (ISO-NE) (Maslennikov, Wang and Litvinov 2017). When an oscillation is detected at ISO-NE, the DEF is calculated at several points within the system. Measurements are mapped to the system's one-line diagram, allowing the source to be identified. Depending on whether the source is within the ISO-NE footprint and if it is monitored by a PMU, the output of the ISO-NE tool may specify the exact source, the region of the ISO-NE system containing the source, or from which adjacent utility the oscillation is coming. Note that in the latter case, the adjacent utility may not contain the source; the oscillation may be traveling through from another region.

In ESAMS, the concept of the ISO-NE tool will be applied at the interconnection level to provide a wide-area view of how the oscillation is moving through the system and to identify the region from where it is originating. At the scale of an interconnection, it would be infeasible to identify the specific generator causing the oscillation. Even if utilities were willing to make the necessary one-line diagrams available, it would be nearly impossible to ensure that they accurately reflect current system conditions. In addition, localization to a specific generator would require vast amounts of synchrophasor measurements to be shared to a central location. As will be discussed shortly, localization to a region only requires measurements at the boundaries between regions to be shared. Localization to a region provides valuable information to operators, both in preventing unnecessary control actions in regions not containing the source and in spurring further analysis within the source region.

The concept for identifying the region containing the oscillation's source is illustrated in Figure 1. Each region represents a logical boundary within an interconnection, .e.g., a balancing authority or reliability coordinator. The arrows represent the flow of oscillation energy (as calculated by the DEF) across the major tie-lines connecting regions. In Figure 1, Region 3 can readily be identified as the area containing the oscillation source because it is producing large amounts of oscillation energy. Practical cases are often less obvious due to the complexity of the system and variability in the DEF estimates.

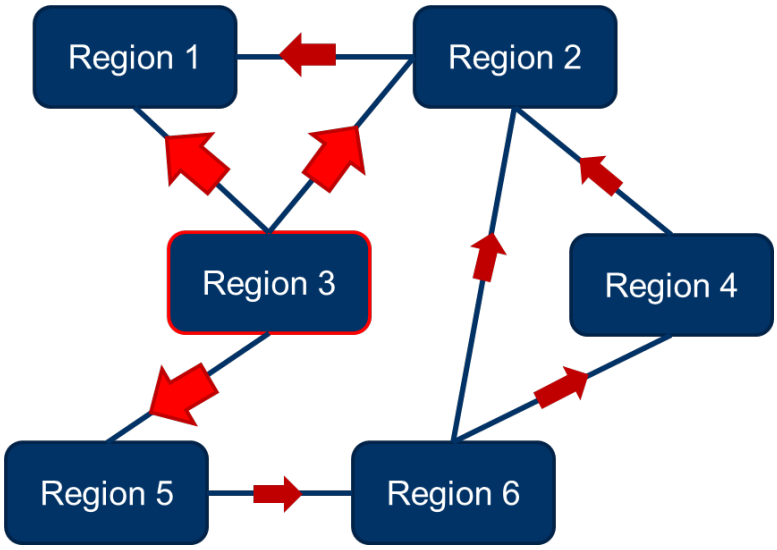

Figure 1. Conceptual illustration of regional oscillation source localization.

In preparation for automating the source identification process, three different criteria were tested. In the first approach, the oscillation energy flowing into (negative) and out of (positive) a region are summed, and regions with a net positive value are identified as possible sources. This approach assumes that all non-source regions will dissipate oscillation energy, leading to negative net values. In practice, this approach was found to be sensitive to variability in the DEF estimates. The approach frequently resulted in multiple regions being identified as possible sources and is not considered further in this report. In the second approach, the net DEF value is again calculated for each region, but only the region with the largest resulting value is identified as a source. This criterion will be referred to as the *max net* criterion. In the third approach, regions that exclusively export oscillation energy (positive DEF) on their tie-lines are identified as possible sources. This criterion will be referred to as the *export* criterion.

To test the criteria and the DEF estimation method proposed in the previous section, they were applied to the cases in a publicly available test case library (Maslennikov, Wang and Zhang, et al. 2016). The library is composed of both simulated and field-measured datasets. Simulated data was generated using a 179-bus simplified model of the Western Electricity Coordinating Council (WECC) system (Sun, Hur and Zhang 2011). Figure 2 presents the one-line diagram of the 179-bus system. The figure also indicates the seven regions considered for testing, the sites of PMUs at the region boundaries, and generators where oscillations originated. Note that for this simplified model only seven PMUs are necessary. More PMUs would be required for the actual WECC system, but the approach could still be implemented practically.

The simulated datasets are divided between natural and forced oscillations. Natural oscillations are inherent to power systems and thus always present. They are typically well damped and not a cause for concern, but certain system conditions and poor tuning of control systems can lead to sustained or growing oscillations. In contrast, forced oscillations arise when malfunctioning or misoperating equipment applies a periodic disturbance to the system. It is important for oscillation source localization algorithms to perform effectively for both types of oscillations.

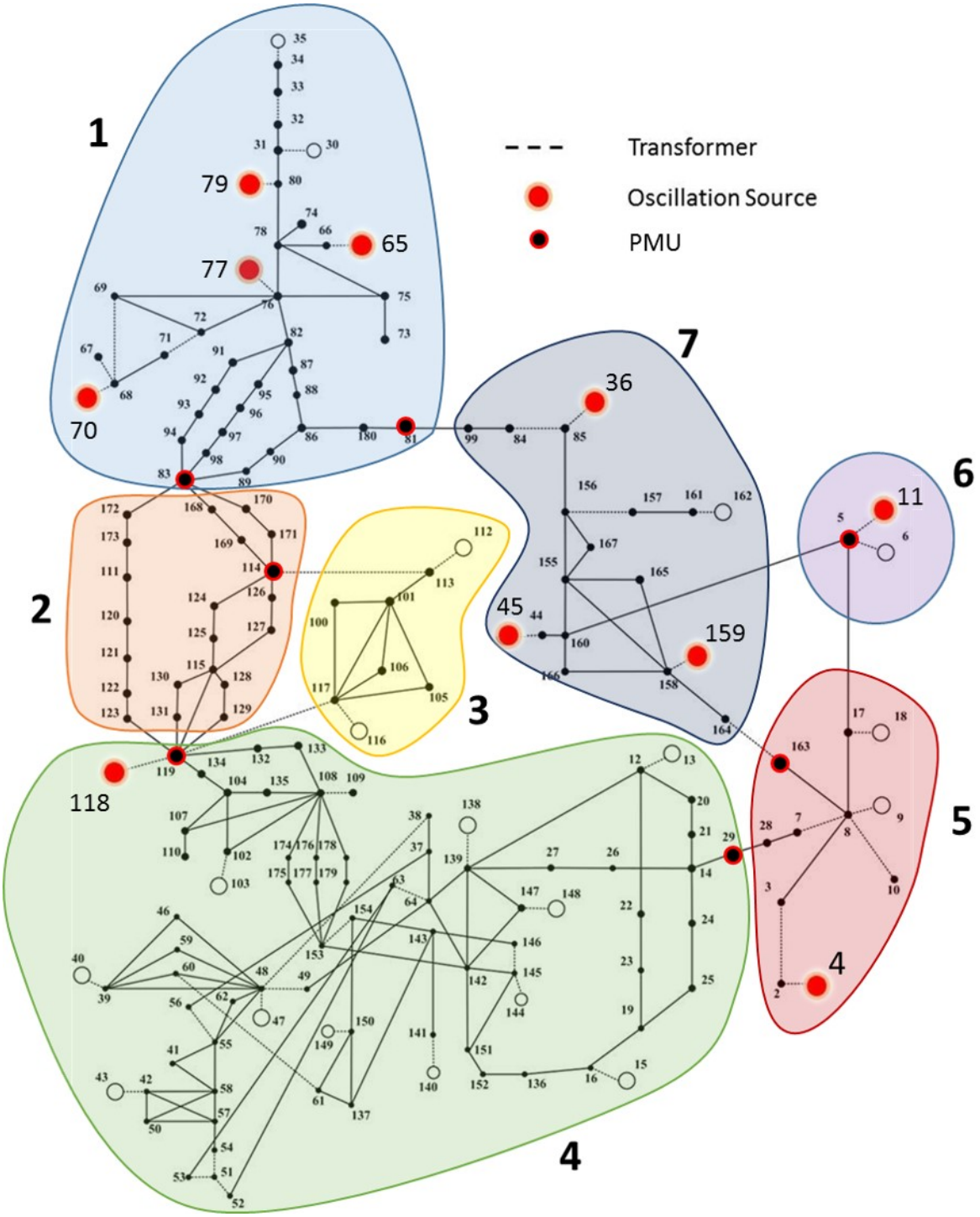

Figure 2. One-line diagram of the 179-bus model with seven defined regions.

Results from the simulated cases are presented in Table 1 (natural oscillations) and Table 2 (forced oscillations). The entries in the *Case* column match those in (Maslennikov, Wang and

Zhang, et al. 2016). The final six cases in Table 2 were added to the test case library following the publication of (Maslennikov, Wang and Zhang, et al. 2016). The entries in the *Generator* and *Region* columns match those in Figure 2. The *Max Net* and *Export* columns correspond to the two previously described criteria for identifying the source region. The *Direct* column refers to calculation of the DEF as in (Maslennikov, Wang and Litvinov 2017), while the *DFT* column refers to calculation as proposed in Section 2.0. To simplify the table, check marks indicate that the source region was correctly identified. Cells in the table are left empty where no region met the criterion. If the wrong or multiple regions met the criterion, the identified regions are listed.

The results presented in these tables are very encouraging. The direct and DFT-based algorithms for calculating the DEF provide nearly identical results. In addition, the *max net* criterion identifies the correct region in nearly every case. The only errors for natural oscillations occur for oscillations at 1.63 Hz. This frequency is beyond the range where the power system's dynamics cause the oscillation to become widespread. Thus, it is a local oscillation. ESAMS is not intended for local phenomena. Rather, it is targeted specifically at oscillations with impact at the interconnection scale. For forced oscillations, the only discrepancy is in case F_7_2, which involves generators in two different regions causing oscillations at identical frequencies. The algorithm is only designed to detect one region, which it does accurately, so this constitutes a gap in the algorithm's ability. However, this type of event would be extremely rare.

The *export* criterion also leads to correct results in most cases, but far fewer than the *max net* criterion. This can be readily explained. Note that the *max net* criterion always leads to the identification of a single region because it is based on the maximum net DEF. In contrast, the *export* criterion can be met by multiple or no regions. These cases may occur because of estimation error in the DEF values. They may also occur if the oscillation energy flows in a loop. For example, consider the oscillations in cases F_5_1, F_5_2, and F_5_3, which originated in region 1 (see Figure 2). Examination of results from these cases showed that significant oscillation energy flowed from region 1 to region 2, but a small amount also flowed from region 7 to region 1. As a consequence, region 1 was not exclusively an exporter of oscillation energy and was eliminated as the potential source region. Ignoring DEF values below a threshold could potentially improve the performance of the *export* criterion, but it is not clear where this threshold should be set. Based on these results, the *max net* criterion appears to be more robust than the *export* criterion.

Table 1. Results of the regional oscillation source localization algorithm applied to simulated natural oscllation cases.

Case	Frequency (Hz)	Generator	Region	Max Net		Export	
				Direct	DFT	Direct	DFT
PD_1	1.41	45	7	✓	✓		
PD_2	0.37	65	1	✓	✓		
PD_3	0.46	11	6	✓	✓	✓	✓
	0.70			✓	✓	✓	✓
	1.63			1	✓	✓	3, 6
PD_4	0.46	11	6	✓	✓	✓	✓
	0.70			✓	✓	✓	✓
	1.63			✓	✓	1, 3, 6	3
PD_5	0.46	11	6	✓	✓	✓	✓
	0.70			✓	✓	✓	✓
	1.63			✓	5	✓	3
PD_6	1.41	45	7	✓	✓		

		159	7				
PD_7	1.41	45	7	✓	✓		
		159	7				
PD_8	1.27	45	7	✓	✓		✓
		36	7				
	1.41	45	7	✓	✓		
		36	7				
PD_9	0.46	11	6	✓	✓	✓	✓
	0.69			✓	✓	✓	✓
	1.63			5	5	1, 5	3

Table 2. Results of the regional oscillation source localization algorithm applied to simulated forced oscllation cases.

Case	Frequency (Hz)	Generator	Region	Max Net		Export	
				Direct	CPSD	Direct	CPSD
F_1	0.86	4	5	✓	✓	✓	✓
F_2	0.86	79	1	✓	✓	✓	✓
F_3	0.37	77	1	✓	✓		
F_4_1	0.81	79	1	✓	✓	✓	✓
F_4_2	0.85	79	1	✓	✓	✓	✓
F_4_3	0.89	79	1	✓	✓	✓	✓
F_5_1	0.42	79	1	✓	✓		
F_5_2	0.46	79	1	✓	✓		
F_5_3	0.50	79	1	✓	✓		
F_6_1	0.1	79	1	✓	✓	✓	
F_6_2	0.1	79	1	✓	✓	✓	✓
F_6_3	0.4	79	1	✓	✓		
F_7_1	0.65	79	1	✓	✓	✓	✓
	0.43	118	4	✓	✓	✓	✓
F_7_2	0.43	70	1	4	4	4	4
		118	4				
FM_1	0.86	4	5	✓	✓	✓	✓
FM_3	0.37	77	1	✓	✓	✓	✓
FM_6_2	0.2	79	1	✓	✓	✓	✓
FM_7_1	0.65	79	1	✓	✓	✓	✓
	0.43	118	4	✓	✓	✓	✓

Field-measured data from the test case library was provided by ISO-NE. Along with the measurements, the dataset includes the simplified system map in Figure 3. For this study, only the tie-lines between ISO-NE (Area 1) and their neighboring utilities (Areas 2 and 3) were considered, i.e., measurements from within the ISO-NE footprint were discarded. Table 3 presents the results for the first three cases in the library. Case 4 was omitted because the true source is unknown, and case 5 was omitted because it was a local event. The DEF values in the table have been scaled to the largest value in the row. Dashes indicate measurements were unavailable for the case. To interpret the results, note that each column corresponds to the oscillation energy flow from one area to another. For example, the *Sub:3:Ln:7* column contains the energy flow from area 1 to area 2. Where values are negative, the energy flows in the

opposite direction. Thus, the results in case 1 indicate that the oscillation energy is flowing from area 2 to1 and from area 1 to 3. This points to area 2 as the source region, in agreement with the information provided in the test case library. Similarly, the results for cases 2 and 3 are in agreement with the sources identified in the test case library. Typically, the DEF values from the direct and DFT-based algorithms are quite similar. The 0.15 Hz oscillation in case 2 is a notable exception, though the discrepancy does not alter the interpretation of the results.

The thorough testing reported here led to the conclusion that the proposed methods could be effectively deployed to identify the source region of oscillations occurring in the EI. The following section provides details on how the methods were implemented in ESAMS.

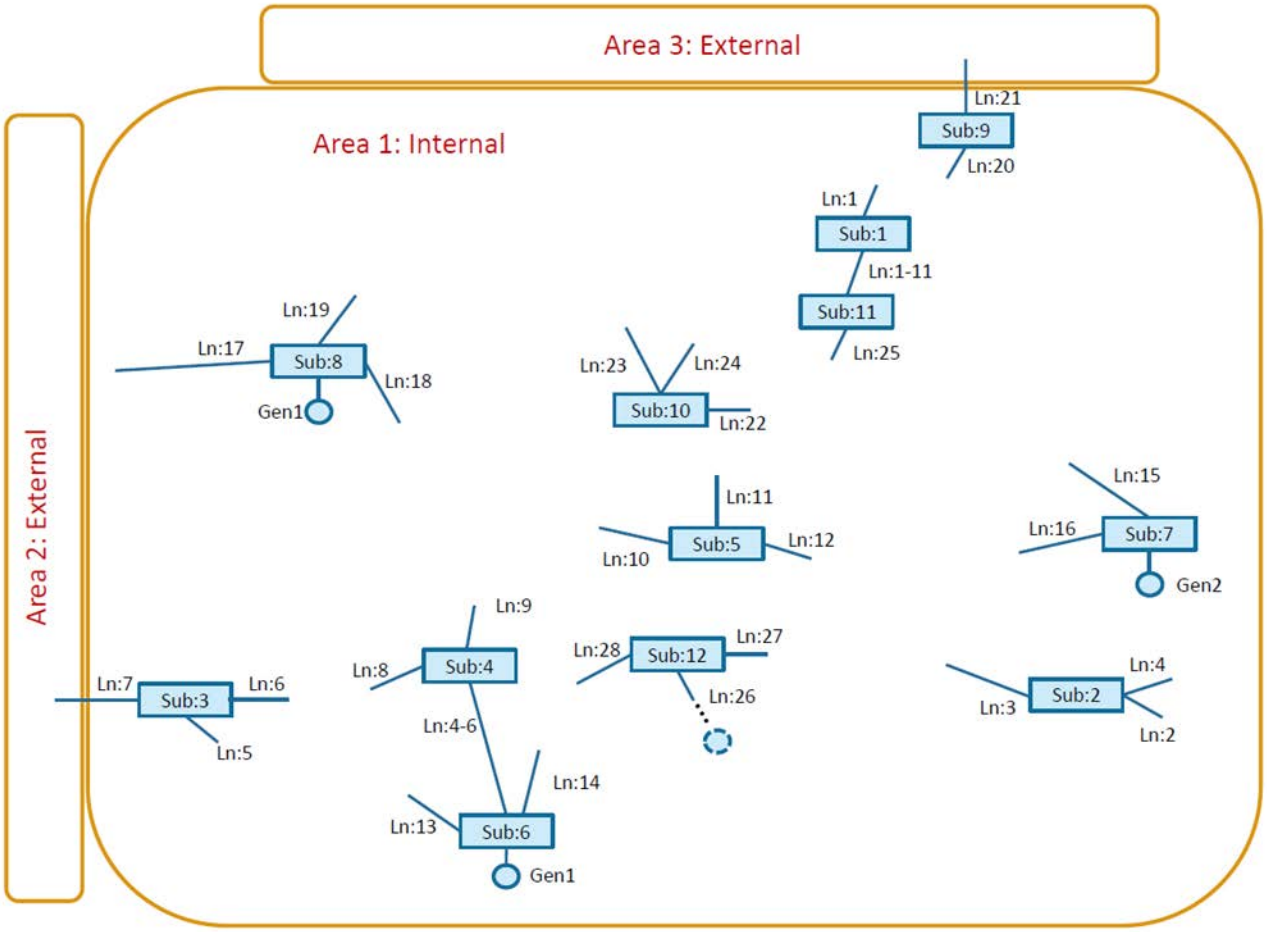

Figure 3. Simplified map of the ISO-NE system.

Table 3. Results of the regional oscillation source localization algorithm applied to measured oscllation cases.

Case	Source	Frequency (Hz)	Method	Sub:3:Ln:7 A1 → A2	Sub:8:Ln:17 A1 → A2	Sub:9:Ln:21 A1 → A3
1	Area 2	0.2745	Direct	-1	-0.78	0.95
			DFT	-0.95	-0.75	1
2	Area 3	0.08	Direct	0.47	--	-1
			DFT	0.75	--	-1
		0.15	Direct	0.36	--	-1
			DFT	1	--	-0.24
		0.3171	Direct	0.41	--	-1
			DFT	0.31	--	-1
3	Area 1	1.13	Direct	1	0.87	0.25
			DFT	1	0.82	0.24

4.0 ESAMS Implementation

ESAMS is being developed as a joint effort between Pacific Northwest National Laboratory (PNNL), Lawrence Berkley National Laboratory (LBNL), and Electric Power Group (EPG). The latter is a vendor specializing in software for electric utilities. The system is comprised of several tools that are coordinated to produce reports of abnormal system conditions. This section describes the integration of the oscillation source localization capability into ESAMS. To begin, an overview of ESAMS is provided.

Figure 4 contains a diagram of the ESAMS platform. Data collected from the Eastern Interconnection Data Sharing Network (EIDSN) (EIDSN, Inc. 2019) is fed into the tool at PJM, the host utility for the ESAMS prototype. EPG's commercial tools DataNXT and RTDMS (Electric Power Group 2019) then flag data quality problems and create signals for analysis, e.g., power flow and voltage angle differences. Signals are then stored in the ESAMS database and retrieved by analysis engines developed by EPG and PNNL. These engines detect system conditions of interest that are reported to users on a regular basis. The remainder of this section describes how oscillation source localization was integrated into PNNL's oscillation analysis module.

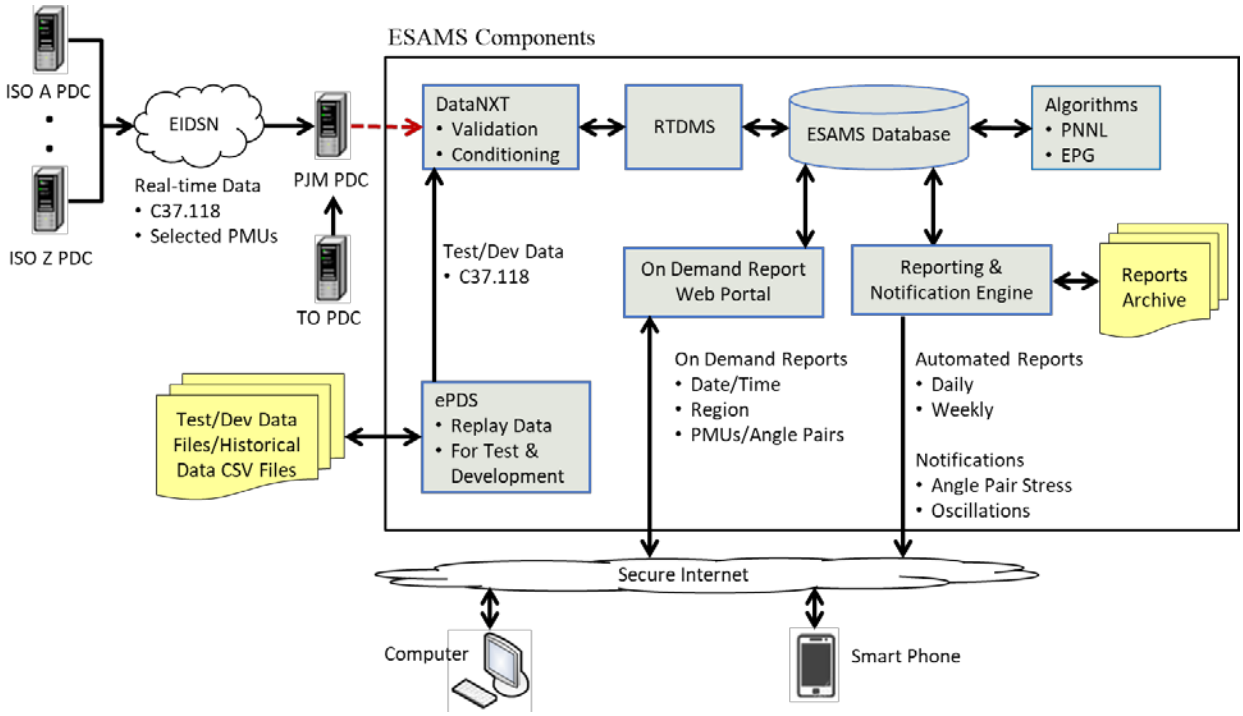

Figure 4. Diagram of the ESAMS tool.

The PNNL oscillation module within ESAMS was written in MATLAB and compiled into an executable. The module reads data from the ESAMS database (see Figure 4) as it becomes available and performs analyses including forced oscillation detection (Follum and Pierre 2016) and natural oscillation baselining (Follum, Amidan and Yin 2018). Each time an oscillation is detected ESAMS records estimates of its frequency and amplitude (Follum and Pierre 2016, Follum and Pierre 2013) in the database. The detector is very sensitive and capable of identifying oscillations with very small amplitudes. The reporting and notification engine in

Figure 4 screens results based on the amplitude to ensure that only oscillations of interest at the interconnection scale are included in reports.

Oscillation source localization was not included in the initial version of the oscillation module because there was ongoing debate within the research community about which algorithms were viable. When the reliability of DEF-based methods was established, the decision was made to incorporate source localization into ESAMS. The January 11 oscillation event in the EI also spurred significant interest in the utility industry and clearly demonstrated the need for a tool to support better coordination during system-wide oscillations.

Within the oscillation module, the new source localization capability was integrated into the existing forced oscillation detection code. After an oscillation is detected, its frequency is passed to the localization algorithm. The DEF estimator described in Section 2.0 is then applied to measurements from each tie-line between regions. The measurements needed for each tie-line are voltage magnitude, voltage angle, active power, and reactive power. As an example from the 179-bus system in Figure 2, the boundary between regions 1 and 2 is associated with the voltage magnitude and angle from bus 83 along with the power flows from bus 83 to buses 168, 170, and 172. Resulting DEF estimates are saved in the database alongside frequency and amplitude estimates for each forced oscillation.

The source localization algorithm described in Section 3.0 is implemented within the ESAMS reporting and notification engine (see Figure 4) using the *net max* criterion (the source is the region with the largest net energy flow). As part of the project's ongoing work, the results will be displayed geographically in the reports generated by ESAMS, providing a clear indication of where an oscillation originates and how its energy flows through the interconnection.

5.0 Conclusion

Since 2008, utilities have made significant progress in the use of synchrophasor measurements within their footprints. However, much could be gained by analyzing measurements from across utility boundaries to a greater extent. The January 11, 2019 oscillation event in the EI clearly demonstrated that cohesive coordination strategies for system-wide events are not in place. The ESAMS tool is an initial step toward establishing coordinated responses that quickly and effectively mitigate oscillations when they occur.

The updated oscillation module within ESAMS is based on the thoroughly tested DEF method. The implementation within ESAMS uses a new expression for the DEF that was derived in Section 2.0. This expression can be evaluated in the frequency domain as to avoid the bandpass filtering necessary for the direct time-domain method. In previous applications, the DEF method has primarily been used to identify the specific generator producing an oscillation. For use at the interconnection scale, a new approach of first localizing an oscillation to a region was introduced in Section 3.0. Results from simulation- and measurement-based studies indicate that the proposed methods reliably indicate the region containing the oscillation's source.

Presently, the new version of the oscillation module described in Section 4.0 is being tested and integrated into ESAMS by EPG. One of the significant remaining challenges is to configure the tool to identify the tie-lines between regions in the EI. This task requires careful coordination with utility partners to ensure that regions are accurately defined and adequate measurements are available. Once the full ESAMS prototype is online, validation will be performed to ensure that results are ready to be reported to partner utilities. If ESAMS is successful and receives support from utilities, the methods proposed in this report could serve as the basis for a future real-time application to support coordination among system operators to effectively detect and mitigate system-wide oscillations when they occur.

6.0 References

Amidan, Brett, Jim Follum, Tianzhixi Yin, and Nicholas Betzsold. 2018. *FY18 Discovery Thru Situational Awareness: Anomalies, Oscillations, and Classification.* PNNL-27812, Richland, WA: Pacific Northwest National Laboratory.

Chen, Lei, Yong Min, and Wei Hu. 2013. "An Energy-Based Method for Location of Power System Oscillation Source." *IEEE Transactions on Power Systems* 828-836.

EIDSN, Inc. 2019. *EIDSN.* Accessed December 9, 2019. eidsn.org.

Electric Power Group. 2019. *Electric Power Group.* Accessed December 9, 2019. http://www.electricpowergroup.com/.

Follum, Jim. 2020. "Statistical Evaluation of New Estimators used in Forced Oscillation Source Localization." *Hawaii International Conference on System Sciences.* Wailea.

Follum, Jim, and John W. Pierre. 2016. "Detection of Periodic Forced Oscillations in Power Systems." *IEEE Transactions on Power Systems* 2423-2433.

—. 2013. "Initial results in the detection and estimation of forced oscillations in power systems." *North American Power Symposium.* Manhattan: IEEE.

Follum, Jim, Brett Amidan, and Tianzhixi Yin. 2018. "A New Spectral Estimator for Identifying Dominant Modes and Detecting Events in Power Systems." *IEEE International Conference on Probabilistic Methods Applied to Power Systems.* Boise: IEEE.

Fritch, Tim. 2019. "EI Oscillation Event." *NASPI.* April 17. Accessed December 3, 2019. https://www.naspi.org/sites/default/files/2019-04/01_nerc_alam_ei_large_oscillation_event_20190417.pdf.

Maslennikov, Slava, Bin Wang, and Eugene Litvinov. 2017. "Locating the Source of Sustained Oscillations by Using PMU Measurements." *IEEE Power and Energy Society General Meeting.* Chicago: IEEE.

Maslennikov, Slava, Bin Wang, Qiang Zhang, Feng Ma, Xiaochuan Luo, Kai Sun, and Eugene Litvinov. 2016. "A Test Cases Library for Methods Locating the Sources of Sustained Oscillations." *IEEE Power and Energy Society General Meeting.* Boston: IEEE.

NASPI Control Room Solutions Task Team. 2016. "Using Synchrophasor Data for Phase Angle Monitoring." NASPI Report. https://www.naspi.org/node/351.

Sun, Kai, Kyeon Hur, and Pei Zhang. 2011. "A New Unified Scheme for Controlled Power System Separation Using Synchronized Phasor Measurements." *IEEE Transactions on Power Systems* 1544 - 1554.

U.S.-Canada Power System Outage Task Force. 2004. "Final Report on the August 14, 2003 Blackout in the United States and Canada: Causes and Recommendations." U.S. Department of Energy Office of Electricity. https://www.energy.gov/oe/office-electricity.

Wang, Bin, and Kai Sun. 2017. "Location Methods of Oscillation Sources in Power Systems: A Survey." *Journal of Modern Power Systems and Clean Energy* 151-159.

Pacific Northwest National Laboratory

902 Battelle Boulevard
P.O. Box 999
Richland, WA 99354
1-888-375-PNNL (7665)

www.pnnl.gov